Inorganic Chemistry

Article

Time-Resolved Spectroscopy of the Metal-to-Metal Charge Transfer Excited State in Dinuclear Cyano-Bridged Mixed-Valence Complexes

Brendan P. Macpherson,[†] Paul V. Bernhardt,*,[†] Andreas Hauser,*,[‡] Stéphane Pagès,[‡] and Eric Vauthey[‡]

Department of Chemistry, University of Queensland, Brisbane, Queensland 4072, Australia, and Department of Physical Chemistry, University of Geneva, Sciences II, 30, Quai Ernest-Ansermet, 1211 Geneva 4, Switzerland

Visible pump–probe spectroscopy has been used to identify and characterize short-lived metal-to-metal charge transfer (MMCT) excited states in a group of cyano-bridged mixed-valence complexes of the formula $[LCo^{III}NCM^{II}(CN)_5]^-$, where L is a pentadentate macrocyclic pentaamine (L^{14}) or triamine-dithiaether (L^{14S}) and M is Fe or Ru. Nanosecond pump–probe spectroscopy on frozen solutions of $[L^{14}Co^{III}NCFe^{II}(CN)_5]^-$ and $[L^{14S}Co^{III}NCFe^{II}(CN)_5]^-$ at 11 K enabled the construction of difference transient absorption spectra that featured a rise in absorbance in the region of 350–400 nm consistent with the generation of the ferricyanide chromophore of the photoexcited complex. The MMCT excited state of the Ru analogue $[L^{14}Co^{III}NCRu^{II}(CN)_5]^-$ was too short-lived to allow its detection. Femtosecond pump–probe spectroscopy on aqueous solutions of $[L^{14}Co^{III}NCFe^{II}(CN)_5]^-$ and $[L^{14S}Co^{III}NCFe^{II}(CN)_5]^-$ at room temperature enabled the lifetimes of their Co^{II}–Fe^{III} MMCT excited states to be determined as 0.8 and 1.3 ps, respectively.

Introduction

According to the Robin and Day classification,[1] class II mixed-valence coordination compounds comprise two complementary redox active centers; one being a reductant (donor, D) and the other an oxidant (acceptor, A) linked by a bridging ligand. The bridging ligand provides a moderate degree of electronic coupling between the two centers such that through-bond metal-to-metal electron transfer is enabled. On the other hand, the degree of electron delocalization between the electronic ground states of the two chromophores is small, that is, the oxidation states of the two metals are distinct as opposed to strongly delocalized class III analogues where the oxidation states and the separate spectroscopic identities of the two connected metal centers are ambiguous.

Class II mixed-valence compounds exhibit the unique property that they are capable of undergoing an optically induced metal-to-metal charge transfer (MMCT) electronic transition. Hush theory[2] has been successfully applied to a large number of class II mixed-valence compounds in an

effort to understand important spectroscopic and electron-transfer processes in these interesting systems.

For asymmetric class II mixed-valence complexes, where the two bridged centers differ in either their metals or their coordination spheres, the MMCT energy (E_{op}) equals the sum of the free energy difference ($-\Delta G°$) between the two "redox isomers", that is, $D_{ox}-A_{red}$ and $D_{red}-A_{ox}$ and the reorganizational energy of the electron-transfer reaction (λ, a sum of both outer- and inner-sphere terms) (eq 1).

$$E_{op} = -\Delta G° + \lambda \qquad (1)$$

The difference between the redox potentials of the donor and acceptor ($\Delta E° = E°_D - E°_A$, each measured electrochemically) can be used to calculate $\Delta G°$ according to eq 2 for a single electronic transition.

$$\Delta G° = -\Delta E° F \qquad (2)$$

In asymmetric mixed-valence compounds, the product of MMCT is inherently unstable and has a measurable, though very short, lifetime. The classical expression for the rate of back-electron transfer is given by eq 3

$$k_{et} = \kappa_{el} \nu_n e^{\frac{-\Delta G^‡}{RT}} \qquad (3)$$

where κ_{el} is the electronic transmission coefficient, ν_n is the

* To whom correspondence should be addressed. E-mail: P.Bernhardt@uq.edu.au (P.V.B.); andreas.hauser@chiphy.unige.ch (A.H.).
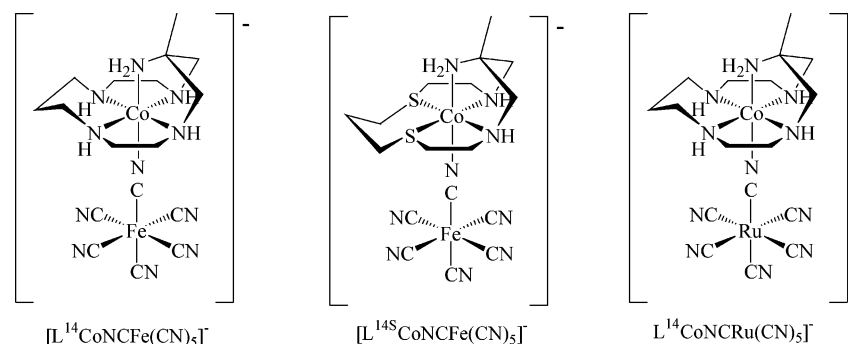† University of Queensland.
‡ University of Geneva.

(1) Robin, M. B.; Day, P. *Adv. Inorg. Chem. Radiochem.* **1967**, *10*, 247–422.
(2) Hush, N. S. *Prog. Inorg. Chem.* **1967**, *8*, 391–444.

Chart 1

$[L^{14}CoNCFe(CN)_5]^-$ $[L^{14S}CoNCFe(CN)_5]^-$ $L^{14}CoNCRu(CN)_5]^-$

nuclear frequency factor, and $\Delta G^{\ddagger}$ is the activation free energy.[3] For a covalently bridged dinuclear complex (where no work term is required to bring the reacting metal centers together), Marcus theory relates $\Delta G^{\ddagger}$ to the free energy change ($\Delta G°$) and the reorganization energy λ (eq 4).[2−4]

$$\Delta G^{\ddagger} = \frac{(\lambda - \Delta G°)^2}{4\lambda} \quad (4)$$

Hence by substitution, variations in the rate of electron transfer may be related to the experimentally derived redox potentials of the D and A centers and E_{op} (according to eq 5).

$$k_{et} = \kappa_{el}\nu_n \exp\left(\left(\frac{-(\lambda - [(E°(A_{ox/red}) - E°(D_{ox/red})]F)^2)}{4RT\lambda}\right)\right) \quad (5)$$

Visible/near-infrared (NIR) pump−probe spectroscopy (on various time scales) has been used successfully to identify and characterize short-lived electronically excited MMCT states.[5−9] Visible pump/IR probe experiments have also identified the importance of vibrational dynamics and solvent effects in the mechanism of relaxation to the ground state during back-electron transfer.[10]

Specifically, the back-electron-transfer reactions of CN-bridged Ru−Ru, Ru−Fe, and Os−Os dinuclear complexes of the general formula $[(H_3N)_5M^{III}NCM'^{II}(CN)_5]^-$ have been the focus of several studies.[5,6,9−14] In some cases, the MMCT excited states in these complexes were probed in the IR region, since the C≡N stretching band is sensitive to the oxidation state of the cyanometalate.

In most cases, the complexes displayed multiexponential decay following MMCT excitation. This was assigned to the formation of a range of vibrationally excited molecules following the back-electron-transfer step. Different lifetimes were observed at different infrared frequencies, indicating that a range of vibrational modes are involved and back-electron transfer was found to be faster than vibrational relaxation.[5,6,9,10,13,14]

The compounds that we have investigated here (Chart 1) are representative of a series of molecular mixed-valence complexes that we have reported in recent years.[15−19] We have chosen pump wavelength to coincide with the MMCT band of each compound, thus initiating intramolecular electron transfer. The probe wavelength has been varied in small intervals and the change in optical density at each increment has enabled the construction of difference spectra, giving spectroscopic information on transient species formed by the excitation pulse.

Experimental Section

Syntheses and Sample Preparation. The syntheses of Na-$[CoL^{14}NCFe(CN)_5]$,[16] Na$[CoL^{14S}NCFe(CN)_5]$,[19] and Na$[CoL^{14}-NCRu(CN)_5]$[19] (Chart 1, all with the macrocycle coordinated in a trans configuration) have been reported. The samples used for nanosecond pump−probe spectroscopy, studied at cryogenic temperatures, were prepared as glasses by using solvent mixtures of 1:1 glycerol/water or 2:1 mixtures of ethylene glycol/water or as KBr pellets, though scattering effects are more significant in the latter case. The samples used in femtosecond experiments at room temperature were prepared as neat aqueous or ethylene glycol solutions.

Equipment. For experiments with nanosecond time resolution, the second harmonic (532 nm) of a Quantel Brilliant Nd:YAG pulsed laser was used to excite into the edge of the MMCT absorption band of the sample held at 11 K in a closed cycle cryostat. A Xe-arc lamp was used for the probe beam with the

(3) Marcus, R. A.; Sutin, N. *Biochim. Biophys. Acta* **1985**, *811*, 265−322.
(4) Marcus, R. A. *Annu. Rev. Phys. Chem.* **1964**, *15*, 155−196.
(5) Walker, G. C.; Barbara, P. F.; Doorn, S. K.; Dong, Y.; Hupp, J. T. *J. Phys. Chem.* **1991**, *95*, 5712−5715.
(6) Kliner, D. A. V.; Tominaga, K.; Walker, G. C.; Barbara, P. F. *J. Am. Chem. Soc.* **1992**, *114*, 8323−8325.
(7) Tominaga, K.; Kliner, D. A. V.; Johnson, A. E.; Levinger, N. E.; Barbara, P. F. *J. Chem. Phys.* **1993**, *98*, 1228−1243.
(8) Reid, P. J.; Silva, C.; Barbara, P. F.; Karki, L.; Hupp, J. T. *J. Phys. Chem.* **1995**, *99*, 2609−2616.
(9) Son, D. H.; Kambhampati, P.; Kee, T. W.; Barbara, P. F. *J. Phys. Chem. A* **2002**, *106*, 4591−4597.
(10) Doorn, S. K.; Dyer, R. B.; Stoutland, P. O.; Woodruff, W. H. *J. Am. Chem. Soc.* **1993**, *115*, 6398−6405.
(11) Wang, C.; Mohney, B. K.; Akhremitchev, B. B.; Walker, G. C. *J. Phys. Chem. A* **2000**, *104*, 4314−4320.
(12) Tivanski, A. V.; Wang, C.; Walker, G. C. *J. Phys. Chem. A* **2003**, *107*, 9051−9058.
(13) Stoutland, P. O.; Doorn, S. K.; Dyer, R. B.; Woodruff, W. H. *Springer Ser. Chem. Phys.* **1994**, *60*, 154−155.
(14) Kambhampati, P.; Son, D. H.; Kee, T. W.; Barbara, P. F. *J. Phys. Chem. A* **2000**, *104*, 10637−10644.
(15) Bernhardt, P. V.; Martinez, M. *Inorg. Chem.* **1999**, *38*, 424−425.
(16) Bernhardt, P. V.; Macpherson, B. P.; Martinez, M. *Inorg. Chem.* **2000**, *39*, 5203−5208.
(17) Bernhardt, P. V.; Macpherson, B. P.; Martinez, M. *J. Chem. Soc., Dalton Trans.* **2002**, 1435−1441.
(18) Bernhardt, P. V.; Bozoglian, F.; Macpherson, B. P.; Martinez, M.; Gonzalez, G.; Sienra, B. *Eur. J. Inorg. Chem.* **2003**, 2512−2518.
(19) Bernhardt, P. V.; Bozoglian, F.; Macpherson, B. P.; Martinez, M. *Dalton Trans.* **2004**, 2582−2587.

wavelength selected using a Spex 270M monochromator (600 grooves/mm holographic grating), fitted with a 532 nm notch filter. A photomultiplier tube (R928 HV, 450 V) connected to a digital oscilloscope (Tektronix TDS 540B) via a fast preamplifier (LeCroy) and triggered by a photodiode in close proximity to the laser was used to measure the transient absorbance. This signal was averaged over 1000−5000 laser pulses. The data were transferred to a computer running LabView, with data manipulation being carried out in IgorPro. Measuring the signal obtained without the probe beam and subtracting this from the signal with the probe beam eliminated interference from the laser electronics, luminescence, and stray light. The transient pulse was converted into absorbance by taking the logarithm of the incident voltage (taken from the average signal before the pulse) over the transient voltage.

Normal absorption spectra were measured by feeding the signal from the photomultiplier through a lock-in amplifier (SR 510) set to the frequency of a chopper placed in the beam of the Xe-arc lamp. A 550 nm cut-off filter was inserted in front of the monochromator for measurements above 600 nm.

Transient absorption measurements performed in the femtosecond time domain were conducted on samples at room temperature. For pumping, a home-built optical parametrical amplifier in noncollinear configuration, generating ultrashort pulses tuneable between 480 and 700 nm, was used. For the experiments reported here, the pump wavelength was centered at 530 nm with spectral bandwidth of 60 nm full width at half-maximum (fwhm), pulse duration of 50 fs, pulse energy of 10 μJ, and 1 kHz repetition rate. Probing at 530 nm was achieved using a portion of the pump pulse, which was deviated along a variable optical delay line. The frequency-doubled output of a standard 1-kHz amplified Ti/sapphire system (Spectra-Physics) was employed for probing at 400 nm. The duration of the pulses at 400 nm was around 100 fs.

The transmitted probe light was detected with a photodiode. To achieve good sensitivity, the pump light was chopped at half of the amplifier frequency, and the transmitted probe−pulse intensity was recorded shot-by-shot and was corrected for intensity fluctuations using a reference signal detected from the front of the sample cell. This results in a resolution on a relative transmission change of less than 10^{-4} under ideal conditions. The fwhm cross-correlation function was around 200 fs. In all three of the experiments, detection was achieved at the magic angle (57.4°).

Results

Nanosecond Pump−Probe Spectroscopy at 11 K. Samples were prepared for low temperature nanosecond pump−probe spectroscopy in solvent mixtures of 1:1 glycerol/water and 2:1 ethylene glycol/water. The MMCT bands were found to be somewhat bathochromically shifted in the solvent mixtures compared to samples prepared in pure water (Supporting Information, Figure S1). Solvatochromism of MMCT bands in class II mixed-valence compounds has been extensively studied.[20] Spectral changes were also observed upon freezing of the samples at 11 K, because of the decrease in temperature and rigid glass formation (Supporting Information, Figure S2). Rigidochromism is observed in polar solvents because of the inability of the dipoles of the solvent molecules to reorient in response to the change in the charge distribution of the excited molecule. Consequently, the excited state is destabilized and a hypsochromic shift of the
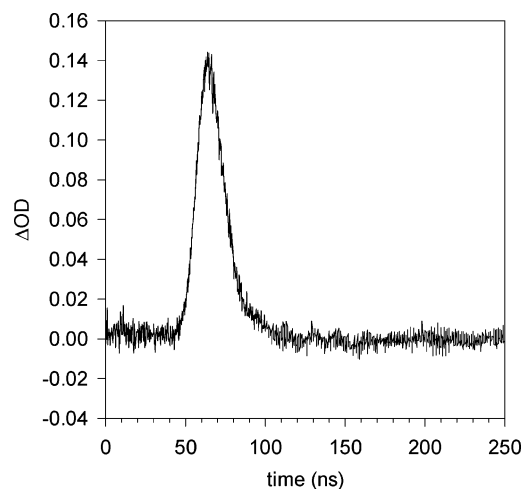
(20) Chen, P.; Meyer, T. J. *Chem. Rev.* **1998**, *98*, 1439−1477.

Figure 1. Time-resolved absorbance change at 370 nm of [L^{14S}CoNCFe-(CN)$_5$]$^-$ in 2:1 ethylene glycol/water at 11 K, 532 nm pump wavelength.

transition results. In rigid media, the outer-sphere contribution to the reorganizational energy (λ_o) may split into the component (λ_{oo}) that is frozen upon glass formation and the component (λ_{oi}) that may still reorient (eq 6).[21]

$$\lambda_o = \lambda_{oo} + \lambda_{oi} \tag{6}$$

The component that is unable to reorient effectively becomes part of the energy gap between the ground and excited states.[20,21] The energy of the MMCT band in these compounds also decreases with increasing temperature.[22] Thus, the changes in temperature and formation of the glass both contribute to the observed spectral changes upon freezing. The spectrum of [L^{14}CoNCFe(CN)$_5$]$^-$ as a KBr pellet at room temperature and 11 K shows a hypsochromic shift of the absorbance bands (Supporting Information, Figure S3). The magnitude of the shift is less than that in the liquid/glass spectra, since in this case only the temperature effect is operational.

A typical time profile of the nanosecond pump−probe experiments using excitation at 532 nm is shown in Figure 1 for [L^{14S}CoNCFe(CN)$_5$]$^-$. From the maximum change in optical density upon excitation (ΔOD) at each probe wavelength, a difference spectrum was constructed, as shown in Figure 2 for [L^{14}CoNCFe(CN)$_5$]$^-$ and in Figure S4 (Supporting Information) for [L^{14S}CoNCFe(CN)$_5$]$^-$. A positive value of ΔOD indicates an increase in absorbance at the probe wavelength; a negative value, in principle, indicates a bleaching. Thus, the spectrum exhibits a strong excited-state absorption at around 350 nm and comparatively weak bleaching at 425 nm. Both peaks appear at wavelengths below the excitation wavelength. Also, the corresponding blank solution in the absence of the complex does not show any transient signals below the pump wavelength. However, a large negative absorbance change at ca. 600 nm was observed in the pump−probe spectrum of the blank solution in the absence (and presence) of the complex. As the solvent mixture does not absorb in this region, and as the negative

(21) Marcus, R. A. *J. Phys. Chem.* **1990**, *94*, 4963−4966.
(22) Macpherson, B. P.; Alzoubi, B. M.; Bernhardt, P. V.; Martínez, M.; Tregloan, P. A.; van Eldik, R. *Dalton Trans.* **2005**, 1459−1467.
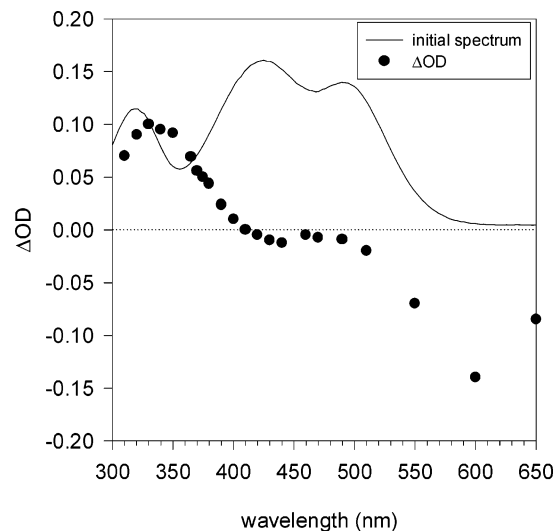
Figure 2. Transient absorbance difference spectrum of $[L^{14}CoNCFe(CN)_5]^-$ in 1:1 glycerol/water (filled circles) and low-temperature absorption spectrum (solid line—arbitrary absorbance): temperature 11 K, pump wavelength 532 nm.

Figure 3. Time-resolved absorbance change at 390 nm of $[L^{14}CoNCFe(CN)_5]^-$ in a KBr pellet: temperature 11 K, pump wavelength 532 nm.

peak is only observed when the probe beam is present, transient bleaching and fluorescence may be ruled out. The peak is thus assigned to stimulated emission from the solvent by the probe beam. Importantly, the blank showed no absorbance changes below 500 nm. In summary, the transient spectrum in Figure 2 is thus only reliable at wavelengths below that of the pump wavelength of the laser, that is, <532 nm.

Ferricyanide ($[Fe(CN)_6]^{3-}$) is known to exhibit a number of electronic transitions in the region 320–420 nm that are significantly more intense than the MMCT transition ($\sim$500 M^{-1} cm^{-1}). As discussed in more detail below, the most prominent feature of the transient absorption spectrum, that is, the rise in ΔOD at $\sim$350 nm, thus corresponds to the population of the transient $[L^{14}Co^{II}NCFe^{III}(CN)_5]^-$ redox isomer. Unfortunately, the above-mentioned spurious "bleaching" seen at 600 nm overlaps significantly with the expected loss of absorbance in the region of the MMCT band because of depopulation of the $[L^{14}Co^{III}NCFe^{II}(CN)_5]^-$ ground state. Nevertheless, the weak negative signal just below the laser line (500–530 nm) indicates that the MMCT band is indeed significantly bleached. Furthermore, the bleaching minimum at 425 nm is in line with the known ground-state absorption band corresponding to a $Co^{III}N_6$ chromophore of this type,[16,22] thus supporting the formation of the transient $[L^{14}Co^{II}NCFe^{III}(CN)_5]^-$ species.

A single-exponential function was fit to the decay of the ΔOD signal. The rate constant was $(9.6 \pm 0.3) \times 10^7$ s^{-1} ($\tau = 10.4$ ns), regardless of probe wavelength. It is apparent that back-electron transfer ($Co^{II} \rightarrow Fe^{III}$) is responsible for the decay to $\Delta OD = 0$, but the time scale of the experiment needs to be considered. The apparent lifetime of the $[L^{14}Co^{II}NCFe^{III}(CN)_5]^-$ transient may actually be governed by the duration of the laser pulse. If the intrinsic lifetime of the transient is shorter than that of the laser pulse, then the decay of the transient signal will merely follow that of the laser. This is in fact what we observe. However, the fact that a transient signal could be observed indicated that the
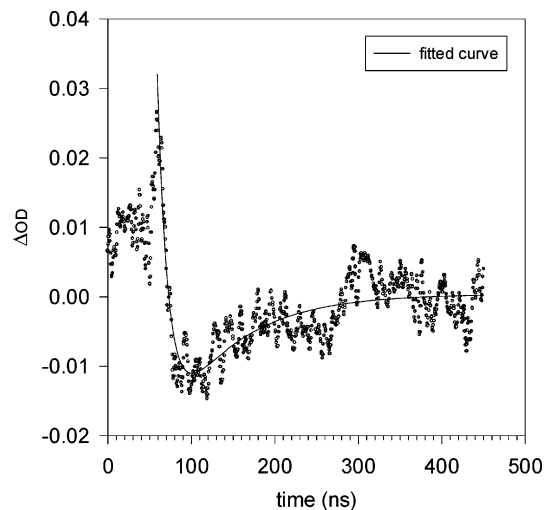
lifetime of the photoinduced state must be of the order of nanoseconds in frozen solution at 11 K. Femtosecond pump–probe spectroscopic experiments (see below) were required to resolve the actual excited-state lifetimes of these compounds.

Pump–probe spectroscopy was also conducted on a sample of $[L^{14}CoNCFe(CN)_5]^-$ prepared as a KBr pellet. As for the frozen solution experiments, a rise in ΔOD in the near-UV (associated with the transient formation of $[L^{14}Co^{II}NCFe^{III}(CN)_5]^-$) is rapidly followed by back-electron transfer (see Figure 3). The transient signals also show a secondary negative ΔOD with a longer lifetime, which was independent of probe wavelength. Overall, the observed response was weaker than that of the glycerol/water mixture owing to the lower optical quality of the sample and light scattering effects from the KBr matrix. Nevertheless, the difference spectrum of the fast component shown in Figure 4 could be collected, showing an increase in absorbance at 350 nm and a decrease in absorbance at around 500 nm.

Attempts to obtain a difference spectrum of $[L^{14}CoNCRu(CN)_5]^-$ at low temperature were unsuccessful when pumped into its MMCT band at 457 nm.

Femtosecond Pump–Probe Spectroscopy at 293 K. Experiments were conducted at room temperature with an experimental setup that allowed resolution on the femtosecond time scale. The solutions of the complex were pumped at 530 nm and probed at either this wavelength or 400 nm. Irradiation into the MMCT band initially causes a bleaching of the intensity of the MMCT absorbance, as is evident from the probing at 530 nm (Figure 5), followed by a return to the ground state. The transient absorbance decay may be adequately reproduced with a double-exponential function, indicating that the return to the ground state takes place via an intermediate state. The data for $[L^{14}CoNCFe(CN)_5]^-$ reveal that the slower component of this decay has a positive ΔOD, indicating an intermediate state with higher absorbance than the ground state. This behavior is not observed in $[L^{14S}CoFe(CN)_5]^-$ (Figure 6), which apparently followed a single-exponential decay. The faster component of the decay

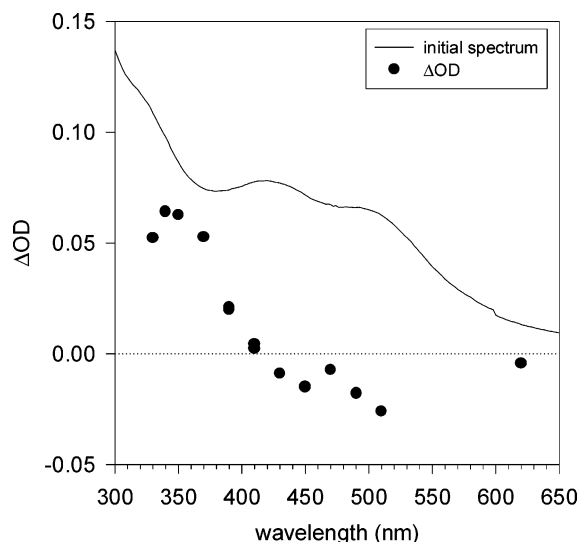**Figure 4.** Transient absorbance difference spectrum of $[L^{14}CoNCFe(CN)_5]^-$ dispersed in a KBr pellet (filled circles) and absorption spectrum (bottom—arbitrary absorbance): temperature 11 K, pump wavelength 532 nm, probe wavelength 390 nm. Spectrum corresponds to the initially formed transient.
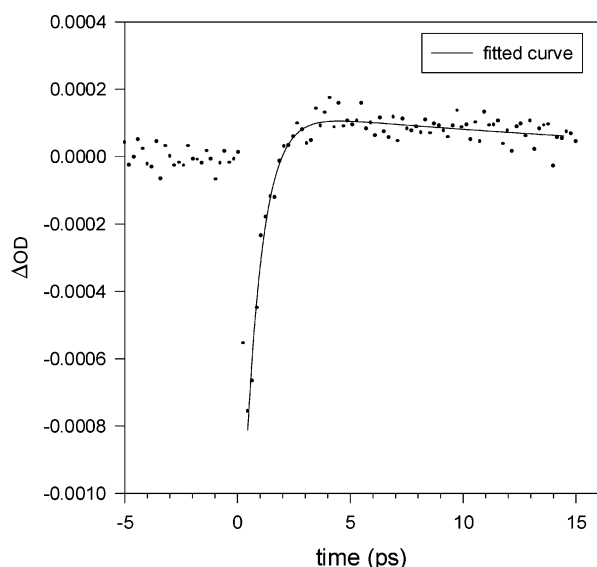

Figure 5. Time-resolved absorbance change at 530 nm of $[L^{14}CoNCFe-(CN)_5]^-$ in water at room temperature, pump wavelength 530 nm. Kinetic parameters obtained from double-exponential model: $\tau_1 = 0.75(3)$ ps (91%) and $\tau_2 = 28(4)$ ps (9%).

for $[L^{14}CoNCFe(CN)_5]^-$ has a shorter lifetime (0.75 ps) than the thioether analogue $[L^{14S}CoFe(CN)_5]^-$ (1.35 ps).

This behavior was not observed in $[L^{14S}CoFe(CN)_5]^-$ (Figure 6), which apparently followed a single-exponential decay. The faster component of the decay for $[L^{14}CoNCFe-(CN)_5]^-$ has a significantly shorter lifetime (750 fs) than that of the thioether analogue $[L^{14S}CoFe(CN)_5]^-$ (1.35 ps).

Probing at 400 nm revealed an increase in absorbance (positive ΔOD) upon irradiation, assigned predominantly to the formation of Fe^{III}, followed by a decrease in absorbance as the complex returned to the ground state. For both $[L^{14}CoNCFe(CN)_5]^-$ and $[L^{14S}CoNCFe(CN)_5]^-$ (Supporting Information, Figures S5 and S6), the faster components have the same time constant, within experimental error, when probed at either 400 or 530 nm.
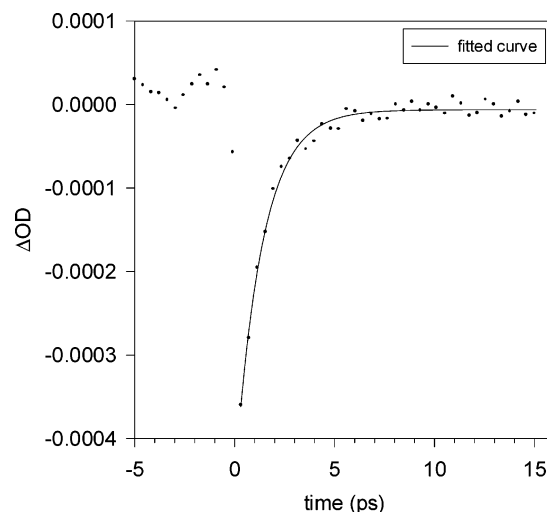
Figure 6. Time-resolved absorbance change at 530 nm of $[L^{14S}CoNCFe-(CN)_5]^-$ in water at room temperature, pump wavelength 530 nm. Kinetic parameters obtained from single-exponential model: $\tau = 1.35(7)$ ps.

The decay rate was also found to be dependent on the solvent. In ethylene glycol, both components of the transient absorbance decay were found to have somewhat longer lifetimes (Supporting Information, Figure S7). Solvent dependence of the rate of back-electron transfer has been observed previously. For example, the time constant for back-electron transfer within the transient $[(H_3N)_5Ru^{II}NCRu^{III}-(CN)_5]^-$ in ethylene glycol is 220 fs, as opposed to 100 fs in water.[14]

Discussion

The difference spectra of $[L^{14}CoNCFe(CN)_5]^-$ and $[L^{14S}CoNCFe(CN)_5]^-$ upon irradiation into the MMCT band show an increase in absorbance peaking at 340 and 390 nm, respectively. Absorption bands due to the formation of the Fe^{III} (ferricyanide) chromophore produced by MMCT excitation would be expected around 326, 395, and 426 nm, when compared to the spectrum of the free complex anion $[Fe(CN)_6]^{3-}$.[23,24] The ΔOD between 400 and 500 nm in the transient absorption spectrum of $[L^{14}CoNCFe(CN)_5]^-$ is weak and negative. Coincidentally, the ferricyanide and $Co^{III}-Fe^{II}$ chromophores exhibit electronic transitions of similar energy and intensity in this region; thus absorbance changes upon excitation are compensatory. The OD increase at 340 nm is consistent with the formation of Fe^{III}, since ferricyanide absorbs more strongly ($\epsilon_{326\,nm} = 876$ M^{-1} cm^{-1}) in this region than ferrocyanide ($\epsilon_{322\,nm} = 345$ M^{-1} cm^{-1}).[24] The electronic spectrum of $[L^{14S}CoNCFe(CN)_5]^-$ displays the tail of an S $\rightarrow Co^{III}$ LMCT band below 330 nm, as seen in analogous thioether cobalt(III) complexes,[25,26] which is significantly diminished upon reduction to Co^{II}. The resulting loss of this

(23) Alexander, J. J.; Gray, H. B. *J. Am. Chem. Soc.* **1968**, *90*, 4260–4271.
(24) Lever, A. B. P. *Inorganic Electronic Spectroscopy*, 2nd ed.; Elsevier: Amsterdam, The Netherlands, 1984.
(25) Osvath, P.; Sargeson, A. M.; McAuley, A.; Mendelez, R. E.; Subramanian, S.; Zaworotko, M. J.; Broge, L. *Inorg. Chem.* **1999**, *38*, 3634–3643.
(26) Gahan, L. R.; Hambley, T. W.; Sargeson, A. M.; Snow, M. R. *Inorg. Chem.* **1982**, *21*, 2699–2706.

Table 1. Excited State Lifetimes of Some Cyano-Bridged Complexes

complex (excited state)	room temp excited-state lifetime (τ) (fs)	ref
$[(NH_3)_5Ru^{II}NCRu^{III}(CN)_5]^-$	85	7–9
$[(NH_3)_5Ru^{II}NCFe^{III}(CN)_5]^-$	89	5
$[(NH_3)_5Os^{II}NCOs^{III}(CN)_5]^-$	<500	10
$[L^{14}Co^{II}NCFe^{III}(CN)_5]^-$	750	this work
$[L^{14S}Co^{II}NCFe^{III}(CN)_5]^-$	1300	this work
$[L^{14}Co^{II}NCRu^{III}(CN)_5]^-$	not observed	this work

band and growth of the ferricyanide absorption band lead to a shift in the difference spectrum maximum to longer wavelength compared with the pentaamine analogue. In addition, the greater absorptivity of the Co^{II} bands of the thioether complex around 400 nm results in a positive ΔOD at this region, because of the combination of the loss of Co^{III} bands and the growth of Fe^{III} and Co^{II} bands.

The femtosecond experimental setup allowed probing at only select wavelengths, namely, 400 and 530 nm. Probing at 530 nm revealed a negative ΔOD, resulting from the depopulation of the ground state and a consequent attenuation of the MMCT absorbance. Probing at 400 nm displayed a positive ΔOD, which is ascribed to the Fe^{III} chromophore, as seen in the nanosecond time-scale experiments.

The double-exponential decay kinetics seen in experiments in the femtosecond time domain clearly indicate that decay to the ground state (k_{rel}) takes place via an intermediate with a lifetime on the order of picoseconds, which confirms our conclusion that the apparent decay rate constants determined in the nanosecond time-scale experiments were indeed governed by the lifetime of the pulse and not by intrinsic electron-transfer rates. We reject the possibility that the faster decay process represents intersystem crossing from the initially formed low-spin Co^{II} ($t_{2g}^6 e_g^1$) state to the energetically more favorable high-spin ($t_{2g}^5 e_g^2$) state followed by a slower back-electron transfer to the ground-state $Co^{III}-Fe^{II}$ redox isomer. First, the rates of intersystem crossing for Co^{II} complexes (low-spin/high-spin) at room temperature are generally of the order 0.1–1 ns.[27,28] Furthermore, a change in spin state at the Co^{II} center would be unlikely to have a major influence on the absorbance of the Fe^{III} center. The fact that the fast component of the decay is also observed at 400 nm with an identical lifetime suggests that the fast initial step involves recovery of the electronic ground state, that is, back-electron transfer. Thus, the slower decay is assigned to vibrational relaxation of the $Co^{III}-Fe^{II}$ complex, which is consistent with lifetime measurements on other photoexcited mixed-valence complexes (Table 1).[5,6,9–14]

The intensity of a transient signal will be related to the number of molecules in their excited state (N^1) relative to those that are in their ground state (N^0). When the rate of decay ($N^1 k_{rel}$) is greater than the rate of excitation ($N^0 k_{ex}$), a steady state will be established (eq 7). In this case, where relatively few molecules are in their excited state, the total number of molecules (N^{tot}, a constant) may be substituted for N^0 and the excited state population is merely proportional

to k_{ex}/k_{rel} (eq 7).

$$N^0 k_{ex} = N^1 k_{rel}$$

$$N^1 = \frac{k_{ex}}{k_{rel}} N^0 \approx \frac{k_{ex}}{k_{rel}} N^{tot} \qquad (7)$$

Note that k_{ex} is dependent on the lifetime of the pulse duration (herein of the order of nanoseconds or femtoseconds depending on the experiment), whereas k_{rel} should be an intrinsic property of the complex. Given that the rates for back-electron transfer at room temperature are $\sim10^{12}$ s^{-1}, the observation of a difference spectrum in the nanosecond domain at low temperature requires some explanation. Although the nanosecond and femtosecond experiments were undertaken at 11 and 293 K, respectively, it seems unlikely that temperature is responsible for a 3 order of magnitude increase in the rate of back-electron transfer. Variable-temperature back-electron-transfer rate measurements on similar mixed-valence complexes such as $[(H_3N)_5Ru^{III}$-$NCRu^{II}(CN)_5]^-$ and $[(H_3N)_5Ru^{III}NCFe^{II}(CN)_5]^-$ have shown that temperature has only a minor influence.[7]

Thus, an alternative mechanism must give rise to the observation of a difference spectrum in the nanosecond experiments. Intersystem crossing (Co^{II}(low-spin)–Fe^{III}(low-spin) to Co^{II}(high-spin)–Fe^{III}(low-spin)) should be slow (0.1–1 ns)[27,28] in comparison to direct back-electron transfer from the Co^{II}(low-spin)–Fe^{III}(low-spin) state; thus the high-spin state is not populated in the femtosecond experiments. However, the pulse width of the laser in the nanosecond experiments is long in comparison to the direct back-electron-transfer rate, and a molecule may be excited a number of times within the duration of a single pulse. Given the higher power of the nanosecond laser pulses, it is possible that a significant population of the longer lived Co^{II}(high-spin)–Fe^{III}(low-spin) state could develop (Figure 7) and that the
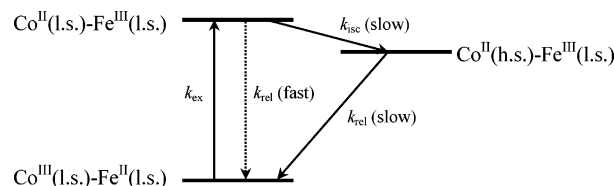
Figure 7. Generation of spin-crossover excited state.

apparent decay we observe may be due to decay (k_{rel} (slow)) from a different excited state. Back-electron transfer from Co^{II}(high-spin)–Fe^{III}(low-spin) to Co^{III}(low-spin)–Fe^{II}(low-spin) is spin forbidden and must be much slower.[29] Furthermore, there is a larger internal reorganizational energy barrier associated with bond length changes at the metal. It is for these reasons that self-exchange rates of hexaamine $Co^{III/II}$ complexes are orders of magnitude slower than reactions of analogous complexes where no change in electronic spin state is required.[29–33] A similarly "slow" back-electron transfer following photoinduced electron transfer has also been

(27) Simmons, M. G.; Wilson, L. J. *Inorg. Chem.* **1977**, *16*, 126–130.
(28) Dose, E. V.; Hoselton, M. A.; Sutin, N.; Tweedle, M. F.; Wilson, L. J. *J. Am. Chem. Soc.* **1978**, *100*, 1141–1147.

(29) Newton, M. D. *J. Phys. Chem.* **1991**, *95*, 30–38.

observed in a mixed valence Co−Ru bipyridine complex, and this was attributed to intersystem crossing.[34]

The intensity of the difference spectrum for the [L^{14S}-CoNCFe(CN)$_5$]$^−$ complex was greater than that of the [L^{14}CoNCFe(CN)$_5$]$^−$ complex. The full extent of the intensity change due to the formation of the Fe^{III} center is obscured by the overlapping charge-transfer band. Since the population of the excited state in the steady-state condition is proportional to the ratio of the rate constants for excitation and relaxation (eq 7), the intensity of the difference spectrum can be expected to reflect relative excited-state lifetimes. Thus, a longer lived excited state of the L^{14S} complex can be inferred, displaying the same order of rates as the femtosecond experiments.

The lifetimes of back-electron transfer from both the high-spin and low-spin states follow the trend of decreasing driving force, which suggests the systems fall within the Marcus "normal" region[35,36] (where $-\Delta G° < \lambda$, eq 4). Furthermore, [L^{14}CoNCRu(CN)$_5$]$^−$, which has a larger back-electron-transfer driving force ($\Delta G°$) and excitation energy (E_{op})[19], did not yield an observable difference spectrum in the nanosecond time domain suggesting a back-electron-transfer rate (eq 5) much faster than that of the other compounds in this series.

Conclusions

The short-lived product of an MMCT transition of three related CN-bridged mixed-valence complexes was investigated by transient absorption spectroscopy on both the nanosecond and femtosecond time scales. Two excited-state redox isomers are present, differing in spin state of the Co^{II} photoproduct depending on the experimental time scale (and pulse width). Back-electron transfer from the low-spin Co^{II} state is rapid (picosecond time scale), whereas the electron transfer from the high-spin Co^{II} center is much slower because of the required spin reorganization and internal bond length (Co−N) changes that accompany electron transfer.

Supporting Information Available: Solvent dependent electronic spectra of Na[L^{14}CoNCFe(CN)$_5$] and Na[L^{14S}CoNCFe(CN)$_5$]; temperature dependent (11 K glass/293 K solution) electronic spectra of Na[L^{14}CoNCFe(CN)$_5$] and Na[L^{14S}CoNCFe(CN)$_5$]; 293 K and 11 K spectra of Na[L^{14}CoNCFe(CN)$_5$] dispersed as a KBr pellet; 11 K nanosecond difference spectrum of Na[L^{14S}CoNCFe-(CN)$_5$] in 2:1 ethylene glycol/water; femtosecond transient absorbance of Na[L^{14}CoNCFe(CN)$_5$] in water at room temperature, probed at 400 and 530 nm; femtosecond transient absorbance of Na[L^{14S}CoNCFe(CN)$_5$] in water at room temperature probed at 400 nm. This material is available free of charge via the Internet at http://pubs.acs.org.

IC0506512

(30) Dubs, R. V.; Gahan, L. R.; Sargeson, A. M. *Inorg. Chem.* **1983**, *22*, 2523−2527.
(31) Brunschwig, B. S.; Ehrenson, S.; Sutin, N. *J. Phys. Chem.* **1986**, *90*, 3657−3668.
(32) Doine, H.; Swaddle, T. W. *Inorg. Chem.* **1991**, *30*, 1858−1862.
(33) Chandrasekhar, S.; McAuley, A. *Inorg. Chem.* **1992**, *31*, 480−487.
(34) Song, X.; Lei, Y.; Van Wallendal, S.; Perkovic, M. W.; Jackman, D. C.; Endicott, J. F.; Rillema, D. P. *J. Phys. Chem.* **1993**, *97*, 3225−3236.
(35) Marcus, R. A. *J. Chem. Phys.* **1965**, *43*, 679−701.
(36) Marcus, R. A. *Faraday Discuss. Chem. Soc.* **1982**, 7−15.